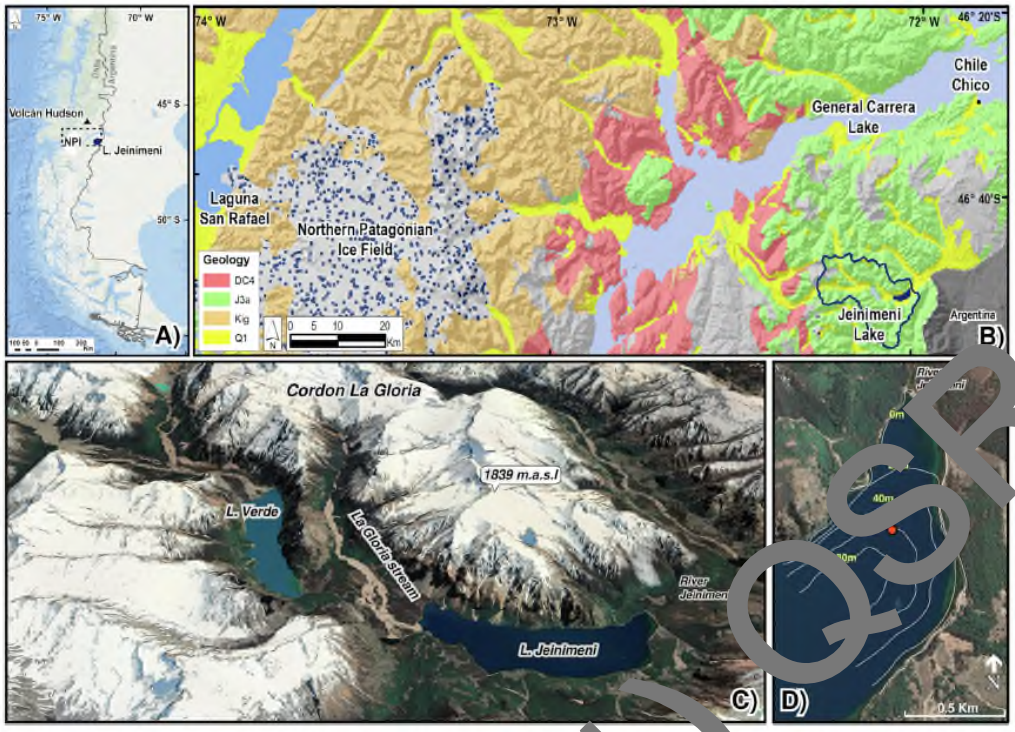

Fig. 1. (A) Location of Lake Jeinimeni within the Aysén region of Chile. The location of the Hudson ...no is reported ...he map. (B) Simplified map of the regional geology, showing the North Patagonian batholith, the Eastern Andean metamorphic complex and the Late ...ass... volcano-sedime...ary Ibañez Formation (Pankhurst et al., 1999). NPI: Northern Patagonian Ice Sheet, LGC/BA: Lago General Carrera/Buenos Aires. Lake Jeinimeni watershed is m...d by a blue c...tour. (C) A lake watershed DEM (Digital Elevation Model) showing the main geomorphological features. The lake water body is reported in ... Map of basic b...metric m...surements and coring site, reported as a red dot, at the northern sector of Lake Jeinimeni. Images C and D, modified from Google Earth© 20... (For in...pretation of the ...eferences to color in this figure legend, the reader is referred to the Web version of this article.)

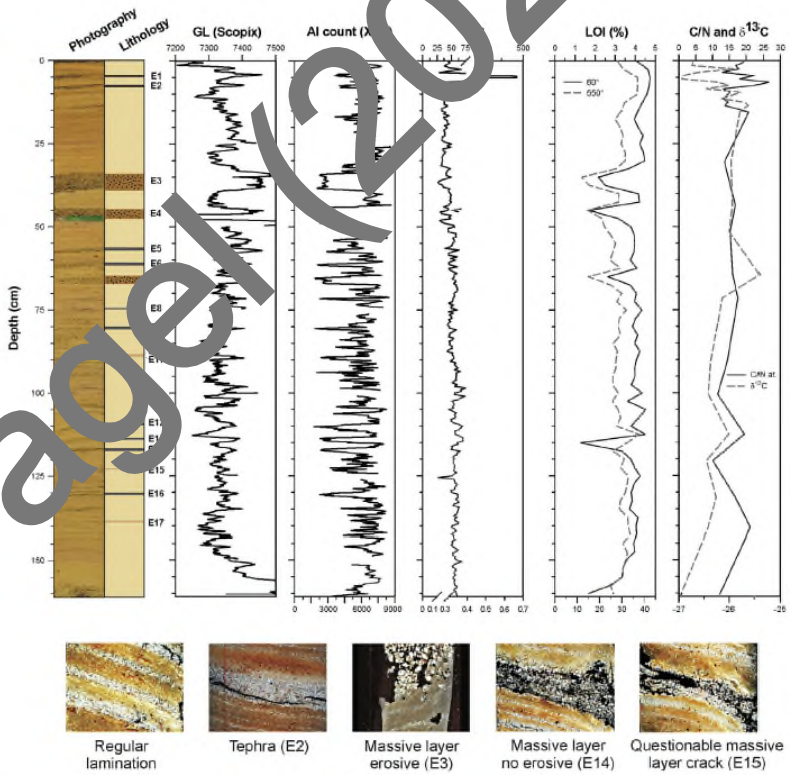

Fig. 2. Core image, simplified lithological column with the event layers depths and major measurements, which include: GL = X-ray grayscale, Al counts, MS = magnetic susceptibility, water (LOI60) and organic matter content (LOI550), carbon/nitrogen atomic ratio (C/N) and carbon stable isotope ($\delta^{13}C$) measurements of core LJe14B. The simplified lithological column indicates the positions of 17 event layers, noted E1 to E17, which interrupt the background sedimentation. The three types of events are plotted with different symbols: the thickest and coarsest layers with erosive base in brown; the coarse layers without any erosion in black; the questionable layer resulting from cracks and sediment deformation in pale brown. E1 at 4.5–5 cm and E2 at 7.4–7.9 cm correspond to two tephras layers. B) Images illustrating the background sedimentation and different event types. The scale of each picture is approx. 20 mm. Note the reported MS curve represents an average of three profiles. (For interpretation of the references to color in this figure legend, the reader is referred to the Web version of this article.)

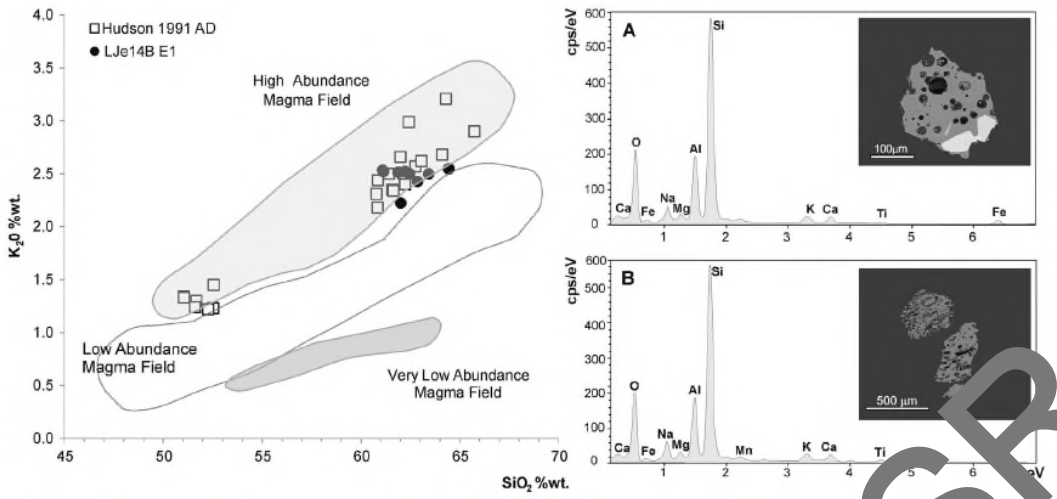

Fig. 3. On the left panel, Electron Microprobe (EMPA) characterisation of glass shards extracted from E1 and E2 event layers in core LJe14B. Al... ...ysed gla... ...s fit with the field of the High Abundance Magma Field of the eruptive products from the Southern Volcanic Zone (SVZ) as reported in Stern et al. (2015). Moreover, the glass c... ...istry is consistent with the signature of the Hudson 1991 eruption (data from (Naranjo and Stern, 2004). On the right panel, Scanning Elec... ...ne ph... ...and elemental EDX composition of representative glassy samples with circular or elongated gas bubbles: A. E1 4.5–5 cm, B - E2 7.4–7.9 cm. The ED... ...major chem... ...of th... ...served glasses from both E1 and E2 layer is consistent with a plagioclase composition.

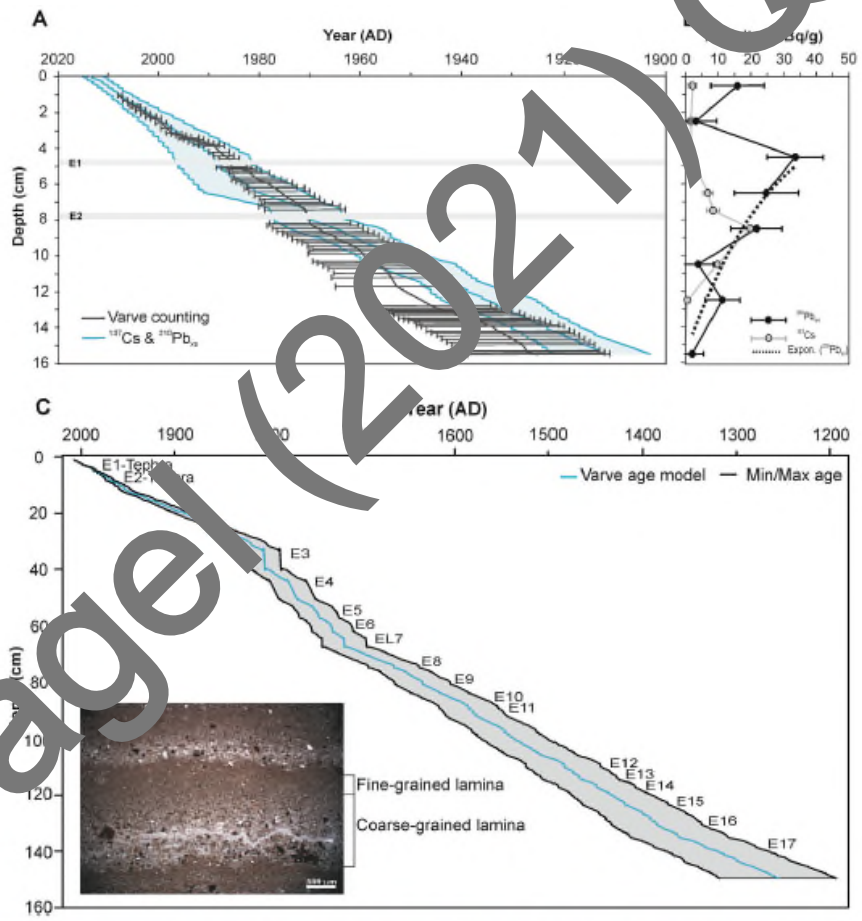

Fig. 4. Age model for the upper 16 cm of core LJe14B. A. Comparison between the age-depth model derived from varve counting and its uncertainty reported as black lines and the age-depth model based on ^{137}Cs and excess ^{210}Pb data and its uncertainty marked as blue lines. For varve counting, maximum age takes in account all varves, minimum age does not include uncertain varves and mean age represents the half of uncertain varves added to chronology. The grey bars indicate events E1 and E2 correspond to the two Hudson eruptions of 1991 and 1971 AD, respectively. B. The curve corresponds to the exponential fit of the $^{210}Pb_{xs}$ decrease. Note the two uppermost samples (0–1 cm and 2–3 cm) and the sample at 7–8 cm (tephra E2) were excluded from the age model since they present no or low $^{210}Pb_{xs}$. The age model derived from ^{137}Cs and excess ^{210}Pb activities (B) is elaborated by linear interpolation with Clam 2.2 code (Blaauw 2010a,b). C. Age model for core LJe14B as derived from varve counting. The events labelled E1 to E17 are marked. The enclosed photo gives an example of the laminated sediment texture, with an alternation of thicker quartz and feldspar-rich coarse-grained lamina and thinner fine-grained lamina. (For interpretation of the references to color in this figure legend, the reader is referred to the Web version of this article.)

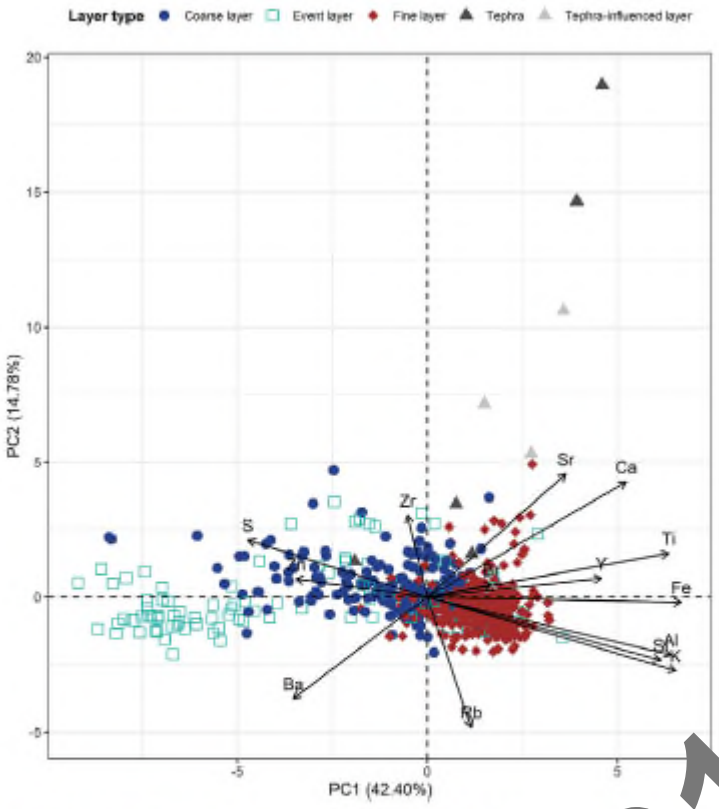

Fig. 5. PCA biplot of XRF core scanner dataset (except Mn) reported as a bivariate diagram of the first two principle components PC1 and PC2. The samples are reported with different symbols according to their dominant lithology. This diagram emphasizes the distribution of the samples in 4 groups according to their lithology. The three groups distributed along the PC1 axis correspond to sediment samples dominated by fine-grained lamina (red diamond), coarse-grained lamina (blue circle) and the massive, sandy to gravely, event E3, E4 and E7 (open blue square). The fourth group plots along the PC2 axis and corresponds to the tephra (dark grey triangle) and tephra-influenced (light grey triangle) layer. (For interpretation of the references to color in this figure legend, the reader is referred to the Web version of this article.)

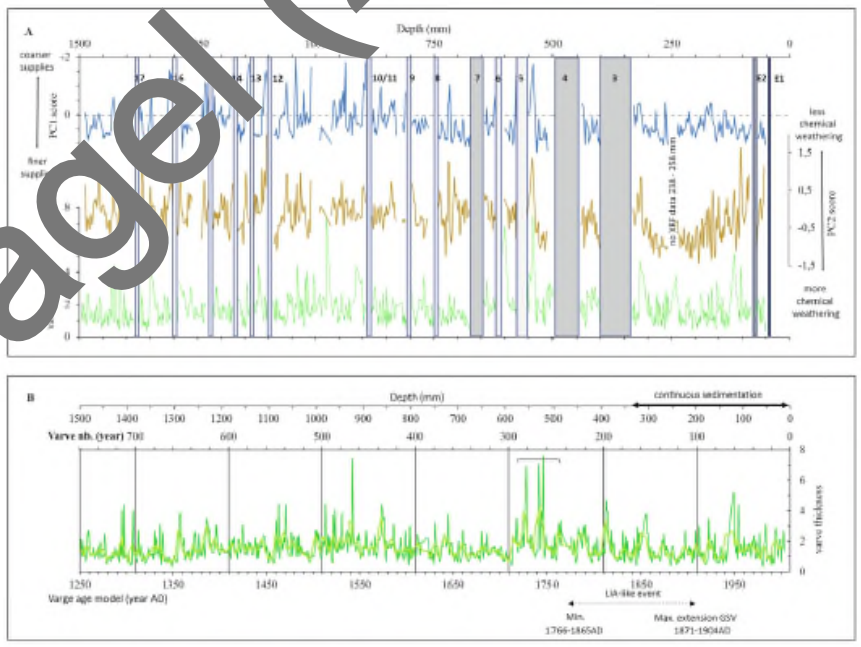

Fig. 6. A. Selected sedimentological and geochemical data of LJe148 reported *vs.* depth, i.e., PC1 and PC2 scores, and varve thickness in mm) The reported numbers correspond to the event layers observed in the core sedimentary features. B. Varve thickness is also reported *vs.* varve number (upper horizontal axis) and varve age model (lower horizontal axis) for comparison. The bold line represents a 5-years moving average curve. The horizontal bar underlines the interval characterized by the thickest varves. Its estimated age ca. 1750 CE is consistent with the oldest limit of the LIA-type event in North Patagonia, as reported by maximal and minimal extension of the Glacier San Rafael (GSR) in the Laguna San Rafael (Araneda et al., 2007). See text for more explanation.

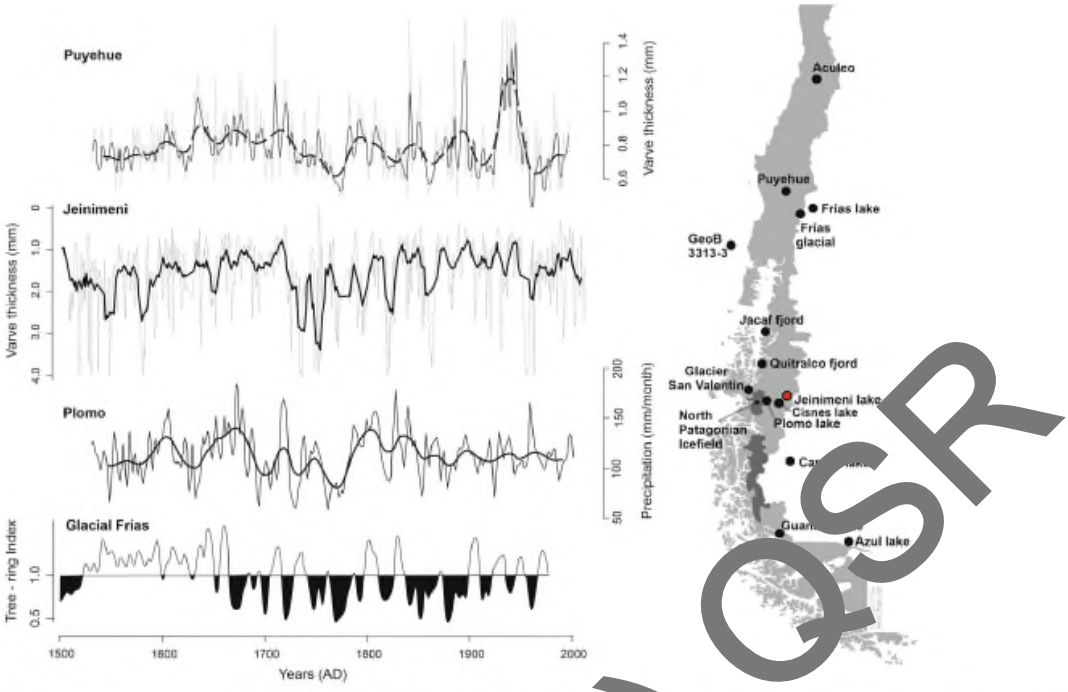

Fig. 7. Comparison of the varve thickness evolution of Lake Jeinimeni LJe14B with some regional records from lacustrine and glacial archives. (a) Varve thickness sequence back to 1530 CE obtained from the short core PUII of Lago Puyehue (40°S) by Boës and Fagel (2008). The varve thickness has been correlated to precipitation, the highest correlation being obtained for May, i.e. autumn/winter transition. The grey line represents the annual variations of the varve thickness, the dashed grey line the 5-year filtered record and, the dashed black line the 30-year filtered. (b) Evolution of varve thickness of LJe14B for the last 500 years. The grey line represents the annual variations of the varve thickness, the black line the 10-year filtered record. (c) Reconstruction of austral winter (JJA) precipitation for varved sediments of Lago Plomo (46° 59′S) derived from mass accumulation rate back to 1530 CE. The thin black line represents 5-year filtered precipitation data. The dashed line shows the 30-year filtered reconstruction. (d) Variations of tree-ring index on *Nothojagus pumilio* over the last 500 years (Villalba et al., 1990). The formation of wider tree-rings has been correlated to cold and rainy summers and to Glacial Frias re-advances. On the curve, the black arrows indicate the position of the Glacier Frias advances, their thickness being indicative of the event extension. Note all the curves indicate higher precipitation upwards. The location of the different records cited in the text is reported on the adjacent map on the right side of the figure. See text for more explanation.